CO_2 IN SOIL GASES OF THE SILALI GEOTHERMAL PROSPECT KENYA

Mulusa G. Igunza, Kipngok Jeremiah, Leakey Auko, Sylvia Malimo, Shilla Chepkemoi, [1]Fridah Mwanyasi, Bett Evans, Isaac Kanda and Luigi Marini
[1]Geothermal Development Company
P.O. Box 17700 – 20100,
Nakuru
KENYA
gigunza@gdc.co.ke

ABSTRACT

The present study is aimed at using probability plots and the partitioning procedure of Sinclair as well as suitable geostatistical tools (e.g., semivariograms and Kriging) in assessing the source of CO_2 in the soil gases of the Silali prospect in the Kenyan Rift. Numerous manifestations occur, in form of hot grounds and fumaroles, in the lower eastern half of the Silali caldera, on the walls of the eastern half of the caldera, and on the eastern outer flanks of the shield volcano. The results of the soil gas survey indicate that most CO_2 anomalies are situated inside the Silali caldera or close to it and there is a close spatial correspondence between most CO_2 anomalies and areas of fumaroles and steaming grounds. This correspondence corroborates the hypothesis concerning the geothermal and structural control on the anomalous population, which is evidently attributable to uprising of deep CO_2-rich geothermal gases towards the surface.

Key words: Silali, CO_2, soil gas, Kenya, caldera, Kenyan Rift Valley.

1. INTRODUCTION

Silali geothermal prospect is located in the East African Rift (Kenya), on the border of Baringo and Turkana Districts, 50km north of Lake Baringo at 1˚10'N, 36˚12'E (Malimo, 2011). The prospect is situated within a semiarid region with typical daytime air temperatures of 35-40˚C. Silali is one of the largest and spectacular volcanoes of the Kenyan Rift, being a broad shield volcano that rises 760m from the rift floor. The most extensive and hot geothermal activity in the prospect occurs in the eastern half of the caldera floor, where a detailed soil gas survey is needed to indicate the active structures which are largely concealed by pumice deposits (Figure 1). Hot altered ground and fumaroles also occur on the walls of the eastern half of the caldera as well as on the eastern outer flanks of the shield volcano (Malimo, 2011).

The assessment of spatial distribution of soil gas anomalies at the surface can give important and interesting information on the origin and processes involving deep and superficial gas species. Soil gas distributions can be directly linked to the evolution of the stress regime as gases migrate preferentially through fractured zones but only along pathways whose permeability has been enhanced by seismic activity and/or through areas of brittle deformation.

Soil gas survey has been proven to be a reliable and simple technique to apply, at different scales, to many geological scenarios (e.g., Annunziatellis et al., 2003; Lewicki et al., 2003; Baubron et al., 2002; De Gregorio et al., 2002; Ciotoli et al., 1998; Ciotoli et al., 1999; Lombardi et al., 1996; Hickman et al., 1995; Duddridge et al., 1991; Durrance and Gregory, 1988; Eremeev et al., 1973). Soil gas distribution can be affected by surface features such as pedological, biogenic and meteorological factors: these are supposed to have only a subordinate effect on gas leakage (Hinkle, 1994). However, it is possible to properly interpret soil gas anomalies and recognize influences of surface features studying the association of different gases (having different origin and physical/chemical behaviour), collecting a large number of samples during periods of stable meteorological and soil moisture conditions (e.g., during dry season) and using appropriate statistical and geostatistical treatment of data (e.g., experimental variograms and Kriging).

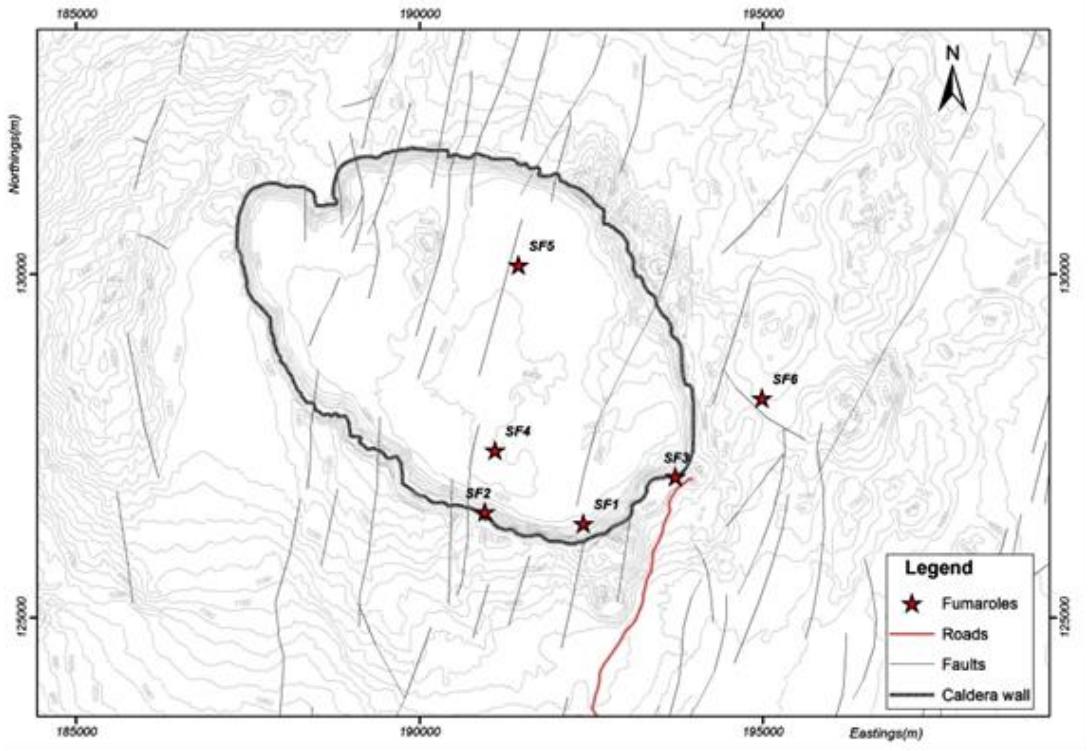

Figure 1: A map of Silali geothermal prospect showing location of Fumarolic discharge points

Field data show the usefulness of the soil gas method for detecting, for instance, crustal discontinuities even when faults are buried or cut non-cohesive clastic rocks which make surface recognition difficult using traditional field methods (Ciotoli et al., 1998; Lombardi et al., 1996; Duddridge et al., 1991; Durrance & Gregory, 1988). These characteristics as well as the rapidity and the low cost of the soil gas survey, make this method a powerful tool for geological investigation.

At Silali volcano, studies on CO_2 concentration in soil gases were carried out by Dunkley et al. (1993), GDC in 2010 as discussed by Malimo (2011) and GDC 2014. In this paper the source of CO_2 is assessed on the basis of probability plots and results correlated with the occurrence of fumaroles and steaming grounds associated with active faults within the Silali prospect.

2. FIELD MEASUREMENTS

The survey was carried out along traverse lines running in an E-W direction (Figure 2). The CO_2 concentration in soil gas was measured using an Orsat apparatus. Gas samples were obtained at a depth of 0.7 m below the surface using a spike, which is equipped with a steel outer jacket to penetrate the ground to the desired depth. The spike is then removed and the outer jacket left inside the hole to allow for the sampling. A stopper with a hosepipe is fixed onto the mouth of the jacket and by using a hand operated vacuum pump, the soil gas is driven into the analytical apparatus. The Orsat apparatus consists of an absorption vessel, which measure about 100 cm^3 and contain 40% KOH solution for absorbing the acidic CO_2. The volume changes in the absorption vessel represent the corresponding amounts of the gases in volumes given as percent of the total gas (Malimo, 2011).

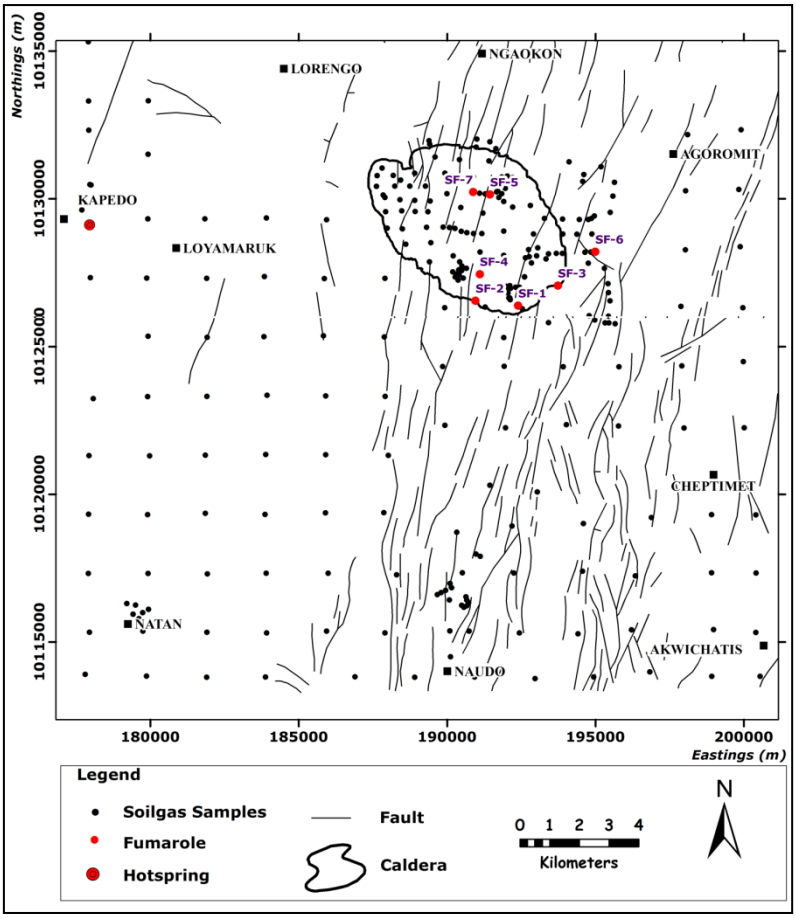

Figure 2: Location map of soil gas sampling points in Silali prospect (Malimo, 2011).

2.1 Data Analysis Methodology

Since soil CO_2 can come from multiple sources (e.g., organic/shallow and geothermal/deep) the Sinclair's (1974, 1976) method is used to separate anomalous values from background values. The method involves the use of probability plots. The probability plot is a simple graphical tool for evaluating the form of the cumulative distribution of a set of numeric data. Probability paper is constructed so that the ordinate is linear or logarithmic as required (i.e., depending on whether the concern is with normal or lognormal distributions); the abscissa is a variable scale arranged so that a cumulative normal distribution plots as a straight line.

If the dataset comprises a unique population, with normal (or lognormal) distribution, the cumulative data define a straight line on a probability (or log-probability) plot. If the dataset has a bimodal distribution (i.e., it is a mixture of two normal or lognormal populations of different averages and partly overlapping intervals), the cumulative data define two linear segments and an intermediate sigmoidal part on a probability (or log-probability) plot. If the dataset has a trimodal distribution (i.e., it is a mixture of three normal or lognormal populations), the cumulative data outline three linear segments alternating with two sigmoidal parts on these plots, and so on.

Partitioning is the procedure used to separate the polymodally-distributed cumulative data into the component populations, based on the position of the inflection point(s), as suggested by Sinclair (1974, 1976). The identification of component populations and their statistical parameters is of utmost importance as each individual population can be assumed to be representative of either a separate process or a distinct geochemical source. Although statistics does not tell us anything on the nature of these different processes and/or geochemical sources, a great step forward in data interpretation is done recognizing that the considered dataset comprises distinct populations and extracting their statistical parameters (e.g., Chiodini et al., 1998 and Ármannsson et al. 2007).

Thresholds between individual populations are adopted in mapping which is performed by means of suitable geostatistical tools such as semivariograms and Kriging.

3. RESULTS AND DISCUSSIONS

The log-probability plot of CO_2 concentration in soil gases for the 247 stations of the Silali prospect dataset is shown in Figure 3 (Marini et al., 2014). The cumulative distribution of CO_2 concentration in soil gases has been partitioned into three individual populations.

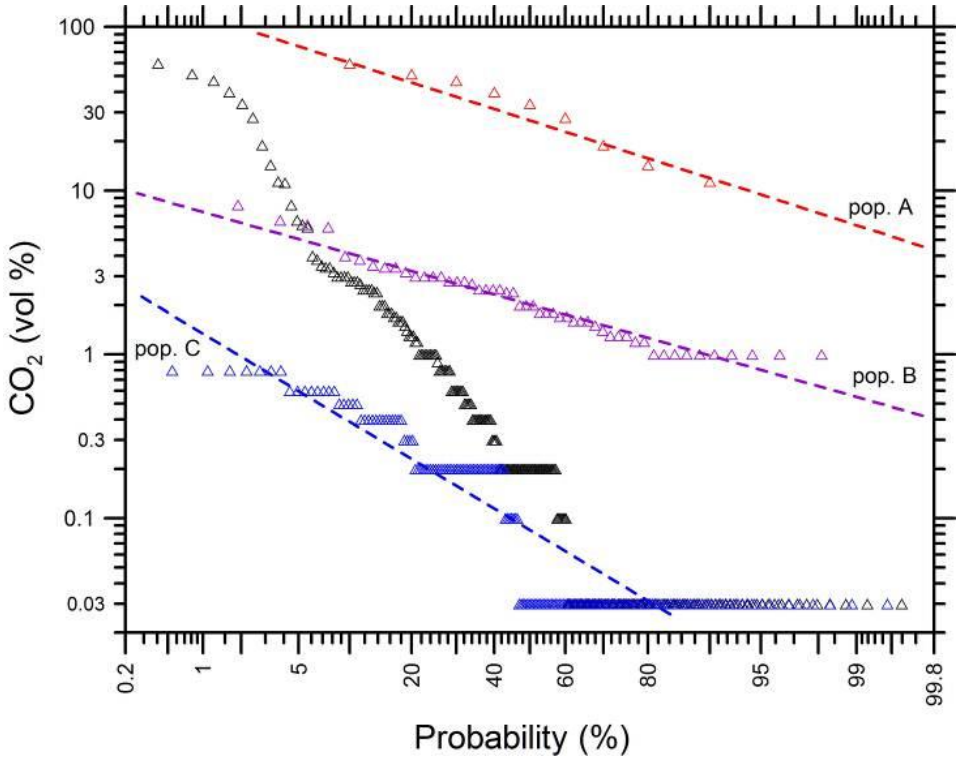

Figure 3: Log-probability plot of CO_2 concentration in soil gases for the 247 stations of the Silali dataset. The black triangles refers to the cumulative distribution of CO_2 concentration, whereas the red, violet and blue triangles identify the three component populations separated adopting the partitioning procedure of Sinclair (1974, 1976). Computed individual populations are represented by dashed lines of the same colors (from Marini et al., 2014).

The high-CO_2 population is called A, the intermediate-CO_2 population is called B and the low-CO_2 population is called C. The threshold between populations A and B is ~10 vol%, whereas the threshold between populations B and C is ~1.1 vol%. The main statistical parameters computed for each component population are given in Table 1.

Table 1: Main statistical parameters for the individual populations (Marini et al., 2014)

Pop.	N	%	Mean	Stand. dev.	Median	Interval	P_{CO2} interval
			vol%	vol%	vol%	vol%	bar
A	10	4.0	32.8	23.0	26.8	>10.0	>0.1
B	29	11.7	2.78	1.47	2.46	1.1-10.0	0.01-0.1
C	208	84.2	0.267	0.52	0.122	<1.1	<0.01

Assuming that total pressure of soil gas is close to the atmospheric pressure, the CO_2 concentrations of 100%, 10%, and 1% by volume correspond to CO_2 partial pressures of 1 bar, 0.1 bar and 0.01 bar, respectively. Therefore, the low-CO_2 population C has P_{CO2} values lower than 0.01 bar. Interestingly, this upper threshold of the low-CO_2 population is lower than the worldwide maximum soil P_{CO2}, 0.042 bar (Brook et al., 1983), suggesting that the population C is entirely attributed to decay of organic matter and root respiration in soils. Hence, population C can also be termed background population.

The lower limit of the high-CO_2 population is significantly greater than the worldwide maximum soil P_{CO2}, 0.042 bar, indicating that population A is representative of deep CO_2. This deep CO_2 is most likely released through boiling/degassing processes occurring in the upper parts of the geothermal reservoir, evidently present at depth in the Silali area, in correspondence with deep-reaching faults and fractures. These tectonic features act as conduits for the upflow of the deep CO_2-rich gases towards the surface.

Population B is somewhat enigmatic. Although its characteristics are intermediate between those of populations A and C, mixing of deep (geothermal) gases and shallow (background) gases is not expected to produce a separate population. A different process or source must be invoked, but its identification is not obvious. Nevertheless, population B can be considered anomalous.

The standardized semivariogram of the decimal logarithm of CO_2 concentration in soil gases is shown in Figure 4. The adopted spherical semivariogram model has a nugget effect of 0.20, and a range of 500 m. Therefore, no relation seems to exist between stations situated at larger distances.

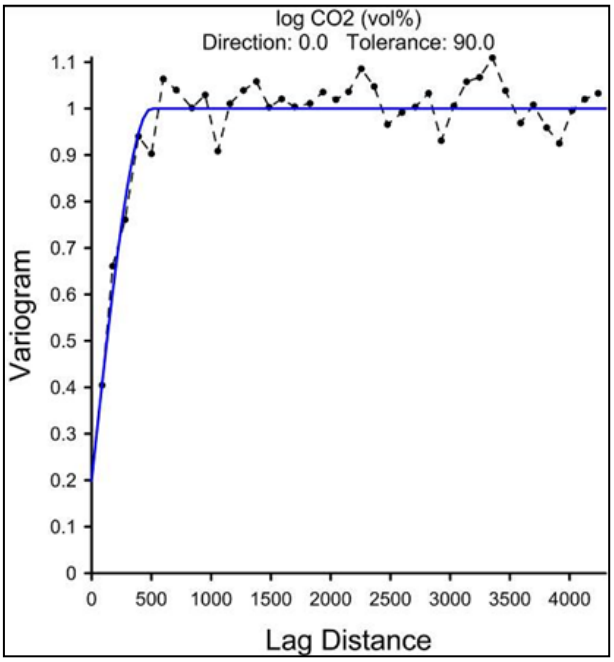

Figure 4: Standardized semivariogram of the decimal logarithm of CO_2 concentration (vol %) in soil gases for the Silali caldera dataset (from Marini et al., 2014).

The continuous-surface map obtained through point Kriging (Figure 5) highlights the presence of high CO_2 concentrations in soil gases, greater than 0.85 vol% and therefore relatable to populations A and B, in the following areas (compare with Figures 1 and 2):

(i) South-eastern part of the caldera near fumaroles/steaming grounds SF-1, SF-2, and SF-3. Three separate highs correspond to each of these fumaroles/steaming grounds but there is a partial lateral continuity between these highs, somewhat shifted to the north. A separate W-E-trending zone of relatively high values is found some hundreds meters further to the north. It connects two areas of steaming grounds, SF4 in the W and another one not coded in the E.

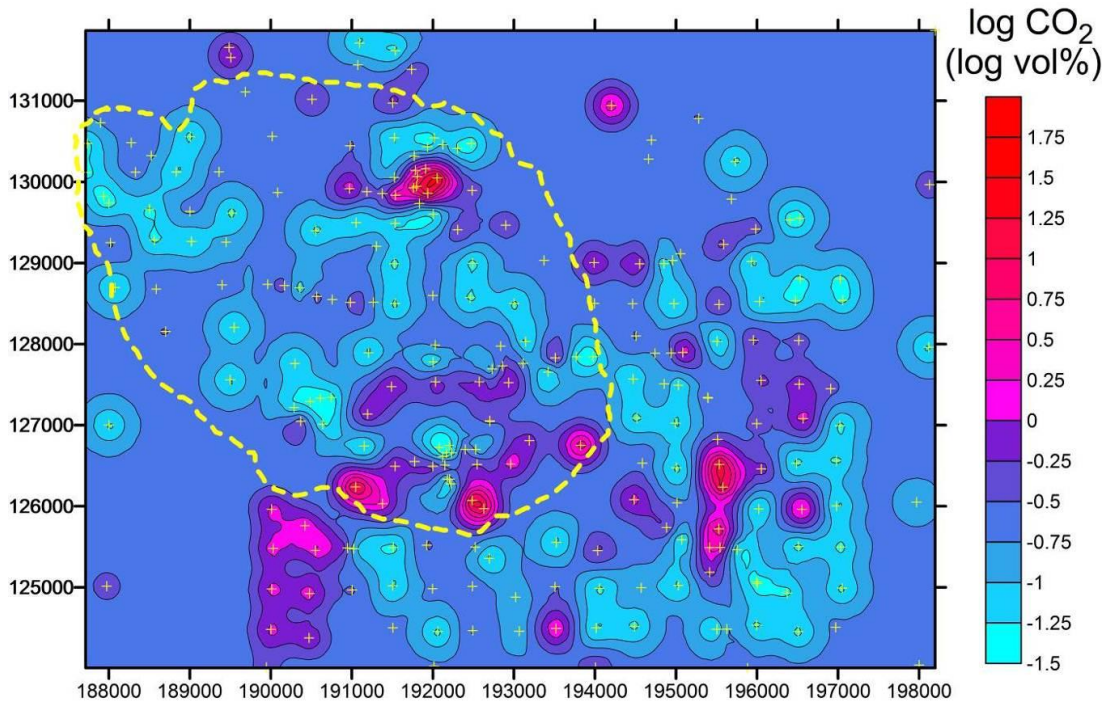

Figure 5: Map of the decimal logarithm of CO_2 concentration (vol %) in soil gases in the Silali caldera and nearby areas (from Marini et al., 2014).

(ii) In the northern sector of the caldera, where a W-E-trending zone of high values connects the fumaroles/steaming grounds SF-5 and SF-7.

(iii) Outside the caldera, to the east of it, at distances higher than 1.0-1.5 km from the caldera rim, where several fumaroles occur (e.g., SF-6). . These high values extend in N-S direction for at least 2 km. Moving further northward the anomaly weakens and widens.

(iv) Outside the caldera, to the south of it. This anomalous area seems to be connected, at least partially, with the high of fumarole/steaming ground SF-2. It extends from the caldera rim for at least 2 km towards the south and for at least 1 km in E-W direction, but its western and southern limits are undefined due to lack of stations.

CONCLUSIONS

Most CO_2 anomalies are situated inside the Silali caldera or close to it and there is a close spatial correspondence between most CO_2 anomalies and areas of fumaroles and steaming grounds. This correspondence confirms the geothermal control on the anomalous population A, which is evidently attributable to uprising of deep CO_2-rich geothermal gases towards the surface, and probably on population B as well.

Assuming that the CO_2 degassing is largely controlled by advective transport along fractures and faults, anomalies of CO_2 concentration in soil gases are expected to exhibit a limited lateral extension from the fracture/fault zones. In agreement with this expectation, the range observed in the semivariogram of Figure 4 is 500 m, indicating that CO_2 concentrations are dependent of one another at distances lower than 500 m.

REFERENCES

Annunziatellis, A.; Ciotoli, G.; Lombardi, S. and Nolasco, F.: Short- and long-term gas hazard: the release of toxic gases in the Albani Hills volcanic area (central Italy). Journal of Geochemical Exploration 77, (2003), 93-108.

Baubron, J. C.; Rigo, A. & Toutain, J. P.: Soil gas profiles as a tool to characterize active tectonic areas: the Jaut Pass example (Pyrenees, France). Earth and Planetary Science Lett, 196, (2002), 69-81.

Baubron, J.C.; Allard, P.; Sabroux, J.C.; Tedesco, D. & Toutain, J.P.: Soil gas emanations as precursory indicators of volcanic eruptions. J. Geol. Soc. London, 148, (1991), 571–576.

Brook G.A., Folkoff M.E., Box E.O. A world model of soil carbon dioxide. Earth Surf. Processes Landforms, 8, (1983), 79-88.

Chiodini G., Cioni R., Guidi M., Raco B., Marini L. (1998) Soil CO_2 flux measurements in volcanic and geothermal areas. Applied Geochemistry, 13, 543-552.

Ciotoli, G.; Etiope, G.; Guerra, M. & Lombardi, S.: The detection of concealed faults in the Ofanto basin using the correlation between soil gas fracture surveys. Tectonophysics, 299 (3–4), (1999), 321–332.

Ciotoli, G.; Guerra, M.; Lombardi, S. & Vittori, E.: Soil gas survey for tracing seismogenic faults: a case-study the Fucino basin (central Italy). J. Geophysics. Res., 103B, (1998), 23781- 23794.

De Gregorio, S.; Diliberto, I.S.; Giammanco, S.; Gurrieri, S. & Valenza, M.: Tectonic control over large-scale diffuse degassing in Eastern Sicily (Italy). Geofluids, 2, (2002), 273– 284.

Duddridge, G. A.; Grainger, P. & Durrance, E. M.: Fault detection using soil gas geochemistry, Q. J. Eng. Geol., 24, (1991), 427-435.

Durrance, E. M. & Gregory, R .G.. Fracture mapping in clays: Soil gas surveys at Down Ampney, Gloucestershire. DOE Report: DOE/RW/88081, Dep. Of Energy, Washington D.C (1988).

Eremeev, A. N.; Sokolov, V.A. & Solovov, A.P.: Application of helium surveying to structural mapping and ore deposit forecasting. In: Geochemical Exploration, 1972, M. J. Jones Ed., pp.183–192, Inst. of Min. and Metall., London (1973).

Hickman, S.; Sibson, R. & Bruhn, R.: Introduction to special section: Mechanical involvement of fluids in faulting. J. Geophysics. Res., 100, (1995), 12,831–12,840.

Hinkle, M.: Environmental conditions affecting concentrations of He, CO_2, O_2 and N_2 in soil gases. Appl. Geochem., 9, (1994), 53– 63.

Irwin, W.P. & Barnes, I.: Tectonic relations of carbon dioxide discharges and earthquakes. J. Geophys. Res., 85, (1980), 3115–3121.

Kerrick, D.M.; McKibben, M.A.; Seward, T.M. and Caldeira, K.: Convective hydrothermal CO_2 emission from high heat flow regions. Chem. Geol., 121, (1995), 285–293.

King, C.Y.; King, B.S.; Evans, W.C. & Zang, W.: Spatial radon anomalies on active faults in California, Appl. Geochem., 11, (1996), 497-510.

Klusman, R.W.: Soil Gas and Related Methods for Natural Resource Exploration. Wiley, Chichester, (1993), 483 pp.

Lewicki, J.L.; Evans, W.C.; Hilley, G.E.; Sorey, M.L.; Rogie, J.D. & Brantley, S.L.: Shallow soil CO_2 flow along the San Andreas and Calaveras Faults, California. Journal of Geophysical Research, 108, (2003), B4, 14 pp.

Lombardi., S.; Etiope, G.; Guerra, M.; Ciotoli, G.; Grainger, P.; Duddridge, G.A.; Gera, F.; Chiantore, V.; Pensieri, R.; Grindrod, P. & Impey, M.. The refinement of soil gas analysis as a geological investigative technique. Final Report. Work carried out under a cost sharing contract with the European Atomic Energy Community in the framework of its 4th R&D program on Management and Storage of Radioactive Waste (1990-1994), Part A, Task 4: Disposal of Radioactive Waste (1996).

Malimo S.J.: Use of radon and carbon dioxide in geochemical exploration - Case study of Silali geothermal prospect, Kenya. GRC Transactions, 35, (2011), 651-656.

Marini L.; Melosh G. & Cumming W.; A review of the geothermal potential of Silali geothermal Prospect and well targeting report; GDC report, (2014), 91 pp.

Rahn, T.A.; Fessenden, J.E. & Wahlen, M.: Flux chamber measurements of anomalous CO_2 emission from the flanks of Mammoth Mountain, California. Geophys. Res. Lett., 23, (1996), 1861–1864
.
Reimer, G.M.: Reconnaissance techniques for determining soil gas radon concentrations: an example from Prince Geoges County, Maryland. Geophys. Res. Lett., (1990), 17, 809– 8012.

Shapiro, M.H. ; Melvin, J.D. ; Tombrello, T.A. ; Fong-Liang, J. ; Gui-Ru, L. ; Mendenhall, M.H. & Rice, A.. Correlated radon and CO2 variations near the San-Andreas fault. Geophys. Res. Lett., 9, (1982), 503–506.

Sinclair A.J. Selection of threshold values in geochemical data using probability graphs. J. Geochem. Explor., 3, (1974), 129-149.

Sugisaki, R.: Origin of hydrogen and carbon dioxide in fault gases and its relation to fault activity. J. Geol., 91, (1983), 239-258.

Sugisaki, R.; Anno, H.; Aedachi, M. & Ui, H.: Geochemical features of gases and rocks along active faults. Geochem. J., 14, (1980), 101–112.

Toutain, J.P. ; Baubron, J.C. ; Le Bronec, J. ; Allard, P. ; Briole, P. ; Marty, B. ; Miele, G. ; Tedesco, D. & Luongo, G.: Continuous monitoring of distal gas emanations at Vulcano, southern Italy. Bull. Volcanol., 54, (1992), 147–155.